ELSEVIER

Chemical Engineering Journal 82 (2001) 291–301

Chemical Engineering Journal

www.elsevier.com/locate/cej

Monte Carlo simulations of the effect of crystallite size on the activity of a supported catalyst

Francisco Gracia, Eduardo E. Wolf*

Department of Chemical Engineering, University of Notre Dame, Notre Dame, 182 Fitzpatrick Hall, IN 46556-5637, USA

Received 19 June 2000; accepted 3 November 2000

Abstract

A dynamic Monte Carlo (MC) simulation is presented for the catalytic reaction $A + \frac{1}{2}B_2 \rightarrow C$. The catalyst surface is modeled as an array of crystallites each one represented as the top projection of a truncated hexagonal pyramid on a flat support. The proportion of corners, edges, base and face atoms or sites varies with crystallite size. The probabilities for the elementary steps comprising the catalytic cycle are calculated from the rate processes at which each elementary step occurs and varies in the different type of sites. We first analyze crystallites of the same size and then a catalyst with a non-uniform distribution of crystallites. The results show that the rate relative to a base case can increase or decrease with crystallite size depending on which elementary step is enhanced in the various types of sites analyzed. Results are relative to parameters used in the base case, which was taken from experimental results for the CO oxidation reaction. Monte Carlo simulations such as the one presented in this paper provide a method of analyzing the effect of crystallite size in the reaction, not available in continuos models. This method is today at the frontier of the modeling of chemical reacting systems and they will enhance our understanding of fundamental issues in catalytic reactions.

Keywords: Crystallite size effects; Monte Carlo

1. Introduction

The traditional approach to kinetic modeling in supported catalysts is via the use of macroscopic rate equations which represents an average of elementary rate processes such as adsorption, desorption surface reaction, occurring in the various crystal faces, edges and corner sites occurring in the myriad of crystallites present on a supported catalyst. Because the surface and the site distribution is affected by the pretreatment and reaction environment, the kinetic constant often change due to changes in pretreatment and reactions conditions [12]. For this reason is difficult to obtain good general activity–structure correlations with experimental results. Microkinetic modeling based on mean field theory kinetic models [7] is an improvement over macroscopic rate equations, but such models are still limited because they do not have the capability to describe the topology of the surface. A review of various theoretical approaches to describe elementary rate processes has been presented by Lombardo and Bell [22]. Among these methods, stochastic models known as Monte Carlo simulations have been extensively used in statistical physics to study systems in equilibrium [3]. Monte Carlo simulations have the capability to account in detail for surface structure and the rate processes associated with them. Dynamic Monte Carlo simulations have been used to follow the evolution of systems over time thus permitting kinetic simulations. Hereafter we will be referring only to dynamic Monte Carlo methods.

One of the first Monte Carlo simulation related to catalysis was reported by Wicke et al. [41] to demonstrate that the Langmuir–Hinshelwood mechanism can lead to the formation of clusters on a single crystal catalyst surface. The Monte Carlo simulation of the L–H mechanism reported by Ziff et al. [47], however, received most of the attention and it is known as the ZGB model. This model was further extended by others to include more details about the surface interactions. Factors such as finite rates of adsorption, desorption and surface reaction [1], diffusion and desorption [15,24], particle–particle interactions [15], lateral interactions between adsorbed species and surface migration [2] and surface defects.

The auto-oscillatory behavior of CO oxidation and other oscillatory reactions have been the subject of numerous experimental and modeling studies and the literature in the field is summarized on various reviews and a book [9,10,37,38]. The reaction occurs via a Langmuir–Hinshelwood (L–H) mechanism and exhibits steady state multiplicity, hysteresis,

* Corresponding author. Tel.: +1-219-631-5897; fax: +1-219-631-8366.
E-mail address: eduardo.e.wolf.1@nd.edu (E.E. Wolf).

1385-8947/01/$ – see front matter
PII: S1385-8947(00)00350-8

Nomenclature

E_i	activation energy for elementary step (kcal/mol)
f_j^p	enhancement or reduction rate factor
k_B	Boltzmann's constant (kcal/K)
k_i	rate constant for elementary step (s^{-1})
M_i	molecular weight of species i
N_s	number of active sites per unit area (sites/cm^2)
P_i	partial pressure of species i (atm)
R	gas constant (kcal/mol/K)
S_i	sticking coefficient of species i (−)
t	time (s)
T	catalyst surface temperature (K)
T_g	bulk gas temperature (K)

Greek letters

θ_i	fraction of sites covered by species i (−)
ρ	density of catalyst support (g/cm^3)

Subscripts

i	1: oxygen, 2: CO, 3: CO_2
j	0: corner site, 1: base site, 2: edge site
p	1: adsorption, 2: desorption, 3: surface reaction

and self-sustained or auto-oscillations. In addition, it has also been found that in single crystals oscillatory behavior is accompanied by spatio-temporal patterns of surface concentration [9,10] whereas on supported catalysts, temperature patterns have been observed during oscillatory behavior [16–18,32,33]. MC simulations are best suited to simulate spatial patterns on surfaces so they have been used to analyze auto-oscillatory behavior due to adsorbate induced surface transformations [8–10,19]. Vlachos et al. [40] used MC simulations of auto-oscillations during CO oxidation and reported that, according to their model, the distribution of surface defects on the catalyst affects the amplitude and period of auto-oscillations. These authors also showed that fluctuations in the thermal environment were important in the transitions between different states of the oscillatory period.

Recently, further details of the interplay of the nanoscale chemistry and kinetics with transport of reactants via the support have been reported by several groups. Zhdanov and Kasemo [44] and Persson et al. [31] simulated the kinetics of an L–H reaction on a crystal with two facets with different reaction rates as well with surface induced reconstruction to simulate oscillatory behavior [45]. McLeod and Gladden [27–29] have simulated the kinetic of hydrocarbon hydrogenation reactions using a Horiouti–Polanyi mechanism and MacLeod used Voronoi tessellation of a surface to simulate crystallites on metal dispersed catalysts [30]. Jansen and colleagues [14,23] have introduced an algorithm used in statistical physics (referred as the master equation) to obtain the correct time dependence for systems with time dependent rate constants. Most of the above papers deal with a single surface with different facets or as in the recent work of McLeod with dispersed catalysts with single rate constants.

Although Monte Carlo simulations have been an effective tool in the simulation of the elementary processes occurring on catalyst surfaces, most of the results reported are limited to reactions on the surface of a single crystal under isothermal conditions. Boudeville and Wolf [4] simulated a temperature programmed reaction on a single crystal with uniform activity during CO oxidation. Our group was among the first to present a Monte Carlo simulation that included factors related to the oscillatory behavior of supported catalysts with multiple crystallites rather than a single crystallite [34]. This model included the basic elementary steps of adsorption, surface reaction, and desorption as the previous studies, but it differs from previous studies in several aspects. To incorporate some of the features of supported catalysts, the model considers several crystallites distributed in some pattern on a non-isothermal supporting surface. Heat transport between crystallites through the support and with the gas phase is included. The model permits to examine microscopic activity features such as the effect of crystallite size as well as macroscopic effects such as thermal communication between the crystallites and their spatial distribution and the effect of different support's properties. It was found that if the rates of the elementary processes remained constant, oscillatory behavior could not be induced by thermal effects only. Auto oscillations were simulated by a mechanism involving oxidation/reduction of the surface leading to the change in sticking coefficients. This mechanism has been proposed by several authors [35] and had been found in agreement between the model and experimental results during CO oxidation over Pd supported catalysts [20,21]. Incorporating the oxidation/reduction model into the Monte Carlo simulation enabled us to study the factors cited above and the effects of thermal communication on the self sustained oscillations.

Van Hardeveld and Hartog [39] argued that when the specific activity changes with crystallite size, it is due to the participation of different type of sites, which depend on the crystallite structure and size. Recent works on Monte Carlo simulations analyze the effect of size, shape or crystallographic faces exposed on a single crystallite supported on a substrate [46]. Our previous work [34] and other papers analyzing supported crystallites (McLeod and Gladen, 1998) [30,31] do not explicitly include in the simulation structural features such as corners, edges or the variation of crystallite size. Thus, the main objective of this work is to study how the differences in activity for different kinds of sites will affect the specific activity of a supported catalyst. This paper incorporates in the simulation the detailed structure of crystallites dispersed on a support with different rates for different sites located in base planes, edges and corners in each crystallite. The effect of varying the crystallite size on the turnover frequency is studied for crystallites with same size as well as with a distribution of crystallite sizes. The surface

is assumed to be isothermal but temperature dependence has been included in the rate constants and no adsorbate-induced transformations are included.

2. Theory

The support is assumed to be a thin square plate with N (1–70) crystallites distributed randomly or in a specified pattern onto it. In a supported catalyst, the crystallites are usually of different size and activity.

2.1. Crystallite model

Following the model proposed by Mavrikakis et al. [25], in this work each crystallite is considered as the top projection of a truncated hexagonal pyramid onto a surface (Fig. 1). Two limiting facets comprise the crystallite, a [1 1 1] plane with sixfold geometry on the top and on three of the six lateral walls, and three [1 0 0] planes with fourfold geometry on the remaining walls of the pyramid. The height of the pyramid is allowed to vary between 2 and 7 layers. The number of atoms, lattice points or sites included in each crystallite varies with its size. We considered that this model was a good representation of a crystallite supported on a substrate. STM micrographs of crystallites on a model catalyst can be closely represented by such a model [6].

The rate processes in both faces are considered equal, whereas those in corner, base and edge sites are computed as follows:

$$R_j^p = f_j^p \cdot R_{\text{face}}^p \quad (1)$$

with j representing the following: 0 is the corner, 1 is the base site and 2 is the edge site. The various rate processes are represented by p with 1 being the adsorption, 2 the desorption, or 3 the reaction. The coefficient f is a factor that accounts for enhancement or reduction in the specific process rate on each type of site. For the case of adsorption, f_j^1 represents changes on the sticking coefficient and varies between 1.99 and 0.1. For adsorption and surface reaction, f_j^p indicates variations on the corresponding rate constant between 10^{-2} and 10^2 times. The probability of the various events occurring on the surface was calculated from the rate constants taken from the literature and our previous work on CO. The relative rates of these processes were changed parametrically by multiplying by the factor f_j^p to ascertain the effects of the structural surface features on the production rate of C. For simplicity we first assumed that the crystallites were all of the same size (uniform crystallite size) and then we assumed a distribution of crystallite sizes on the support.

The reaction $2A + B_2 \rightarrow 2C$ represents a generic form of many catalytic oxidation or hydrogenation reactions. Here we will follow the mechanism corresponding to the CO oxidation reaction but the results can be generalized to reactions with similar stoichiometry. The mechanism of CO oxidation is assumed to occur via an L–H mechanism consisting of the following adsorption, desorption and reaction processes at the catalyst surface.

- A (CO) adsorbs on one catalyst site:

  $$A + S \overset{k_1}{\rightarrow} A \cdot S$$

- Adsorbed A can desorb from the surface:

  $$A \cdot S \overset{k_{-1}}{\rightarrow} A + S$$

- B_2 (oxygen) adsorbs dissociatively on two adjacent sites:

  $$B_2 + 2 \cdot S \overset{k_2}{\rightarrow} 2B \cdot S$$

- Adsorbed A can react with an adsorbed B atom on a neighboring site leading to the product C (CO_2) which desorbs irreversibly very fast relative to the other steps:

  $$A \cdot S + B \cdot S \overset{k_3}{\rightarrow} C + 2S$$

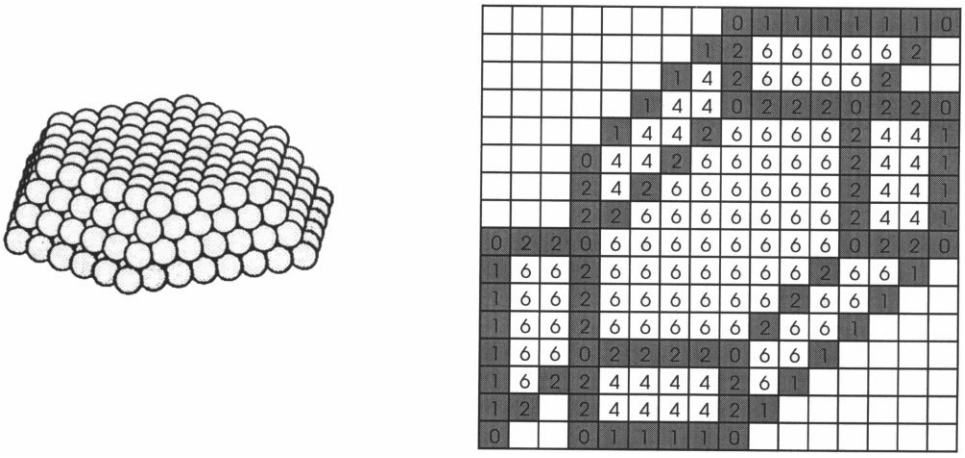

Fig. 1. Crystallite size model and lattice representation. 0: Corner site, 1: base site, 2: edge site, 4: site on [1 0 0] plane with four nearest neighbors (NN) and 6: site on [1 1 1] plane with six NN.

Table 1
Rate expressions used to estimate the event probability

Event	Rate expression[a]	Value used
Adsorption		
$CO + S \xrightarrow{k_1} CO \cdot S$	$k_i = \frac{S_i}{N_s}(2\pi M_i k_B T)^{-1/2}$	$S_1 = 0.5$ (−)
$O_2 + 2S \xrightarrow{k_2} 2O \cdot S$	$r_i = k_i P_i X$	$S_2 = 0.23$ (−)
Desorption		
$CO \cdot S \xrightarrow{k_{-1}} CO + S$	$r_{-1} = k_{-1}\exp(-E_{-1}/RT)$	$k_{-1} = 1.6 \times 10^{-14}$ (s^{-1}), $E_{-1} = 29.0$ (kcal/mol)
Surface reaction		
$CO \cdot S + O S \xrightarrow{k_3} CO_2 + 2S$	$r_{-3} = k_{-3}\exp(-E_{-3}/RT)$	$k_{-3} = 1.0 \times 10^{-12}$ (s^{-1}), $E_{-3} = 10.0$ (kcal/mol)
Event probability for event p in site j on crystallite k	$Y_{jk}^p = p_{jk} f_j^p r_p / \sum_{j=0}^{2}\sum_{p=1}^{3} p_{jk} f_j^p r_p$	

[a] $N_s = 1.2 \times 10^{19}$ (sites/m^2); X is the fraction of neighboring free sites and Ω the fraction of neighboring sites occupied by the co-reactant. P_{jk} is the proportion of site j on crystallite k. Other variables are defined in the nomenclature.

The kinetics constants for each step were taken from a previous work for CO oxidation over Rh catalysts, based mainly on literature values [36]. The rate of desorption of B was not included as a separate step, because at the low temperatures used in the simulations the rate of oxygen desorption is negligible. Likewise, surface diffusion was neglected because the rate parameters used correspond to conditions of high coverage, in which this step is not important. Previous work in our group on Monte Carlo simulations [2] has shown that the effect of CO migration on the surface is inhibited at conditions similar to those considered in this work. Surface diffusion plays a key role in the interpretation of transient behavior for the $CO + \frac{1}{2}O_2$ reaction [46], but this work refers to a more general reaction $aA + bB \rightarrow cC$ and it does not focus on transient phenomena such as oscillatory behavior or reshaping of crystallites. Values of the kinetic parameters along with expression used to calculate probabilities of each event are summarized in Table 1. In our previous work the probabilities were calculated by normalizing the rate of each event by the sum of the rates of all the events occurring on the surface. In this work the probabilities are calculated in a similar way but a weighting factor is included to account for the proportion of each site j on a given crystallite.

The detailed computational procedure of the Monte Carlo simulation can be found in the paper of Araya et al. [1] and the subsequent papers [2,34] and it is briefly summarized as follows:

1. Choose a crystallite randomly among all the crystallites on the support. Then, choose a site randomly among the sites in this crystallite.
2. If the site is empty the probability of the collision (Y_i) of B_2 and A molecule is compared with a random number between 0 and 1 to determine whether A or B_2 is the colliding molecule for this event.

   If the colliding molecule is A, then there are three possibilities following the collision: (i) *no action:* the A molecule bounces back without adsorption or reaction; (ii) *adsorption:* A is adsorbed on that site; and (iii) *reaction:* if a B atom is adsorbed on a neighboring site, then the probability of a reaction event is computed and, if it occurs, two empty sites are generated.

   If the colliding molecule is B_2, then the status of the adjacent sites is checked. Adsorption can occur only when both of the two following conditions are satisfied: (i) at least one neighboring site is empty and (ii) less than half of the neighboring sites are covered by B atoms. The second condition for B_2 adsorption was imposed by experimental results during CO oxidation showing that oxygen only covers a fraction of the surface. A ratio of one oxygen atom to two active sites has been found for chemisorption on supported Pt catalysts [42,43]. Many other experimental and simulation studies also suggest that the maximum oxygen coverage is about 0.5 for the Pt group metal catalysts [5,11,13,26]. Previous MC simulations showed that because of the lack of oxygen desorption, there is oxygen poisoning of the surface as CO desorbs with increasing temperatures [4]. This is not observed experimentally, hence the need for restricting the oxygen coverage if we wish to simulate the behavior real reacting systems such as CO oxidation. When both of the conditions (i) and (ii) are satisfied, a random number is generated to determine whether B_2 adsorption would occur according to the B_2 adsorption. After B_2 adsorption takes place, the neighboring sites of the adsorbed B atoms are searched for an adsorbed A molecule. If an A adsorbed molecule is found, the probability of the surface reaction is tested by another random number. Then, the computational sequence goes back to (1) to start the next trial.
3. If the site is occupied, the choice of the next step (null event, desorption, or reaction) is determined by comparing the probability of each process with a random number between 0 and 1. After the next step is performed, the program goes back to (1) to choose another site. When the procedure in (1) has been performed in all sites of each crystallite and in all crystallites then one Monte Carlo (MC) iteration is completed.

3. Results and discussion

3.1. Uniform crystallite size

To ascertain if the simulation with structured crystallites was consistent with previous results using a square lattice model for a crystallite and with experimental trends observed in previous works [32–34], we conducted our first simulation using crystallites of the same size and the same rate constants in corners, bases, edges and facets (i.e. $f_j^p = 1$, $j = 0, 1, 2$ and $p = 1, 2, 3$). The reaction was simulated on 10 crystallites of 27 Å each, distributed randomly on the support during a temperature programmed reaction (TPR). The reaction rate parameters were calculated for a feed containing 12% B_2, 2% A and 86% of inert. These parameters are similar to the feed composition used in a previous experimental study of CO oxidation over a supported Rh catalyst [32,33]. Each crystallite and the support are at the same temperature, corresponding to isothermal conditions. The simulation started from a clean catalyst surface at 100°C with no A and B_2 adsorbed. After the concentrations of A, B_2, and inert are entered into the program and values of the rate constants are calculated from the expressions given in Table 1, the temperature is increased 1°C every 100 MC iterations. Fig. 2 displays the amount of C produced per MC iteration, and the A and B surface coverage versus the temperature

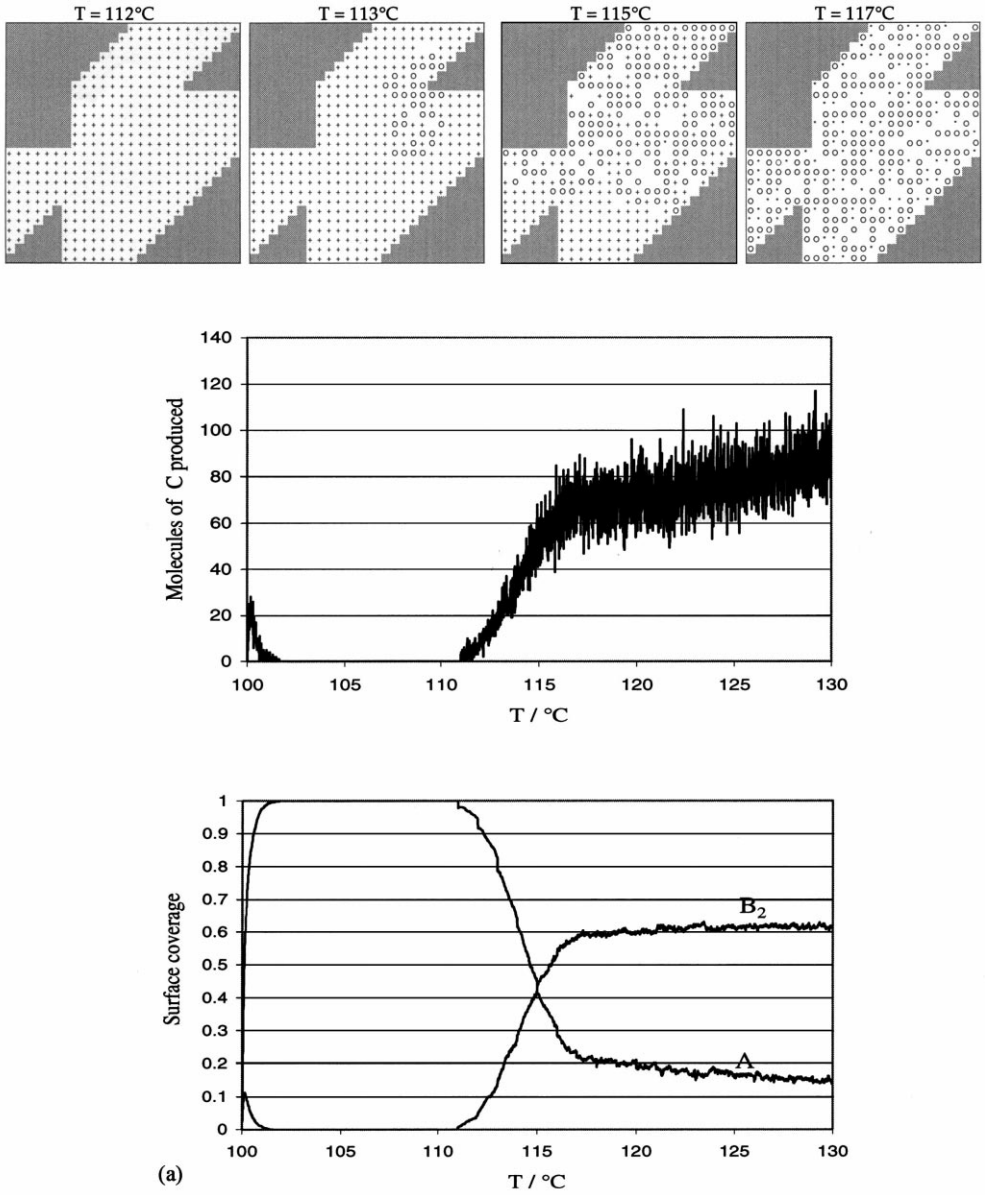

Fig. 2. Simulation of a TPR experiment at 1°C/100 MC iterations on a catalyst with 10 crystallites of the same size (27 Å). Upper panels show maps of the surface coverage at various temperatures. Gray: support; +: A adsorbed; 0: B adsorbed; white: empty site. (a) Increasing ramp started at 100°C showing ignition-like behavior and (b) decreasing ramp starting at 125°C showing extinction-like behavior.

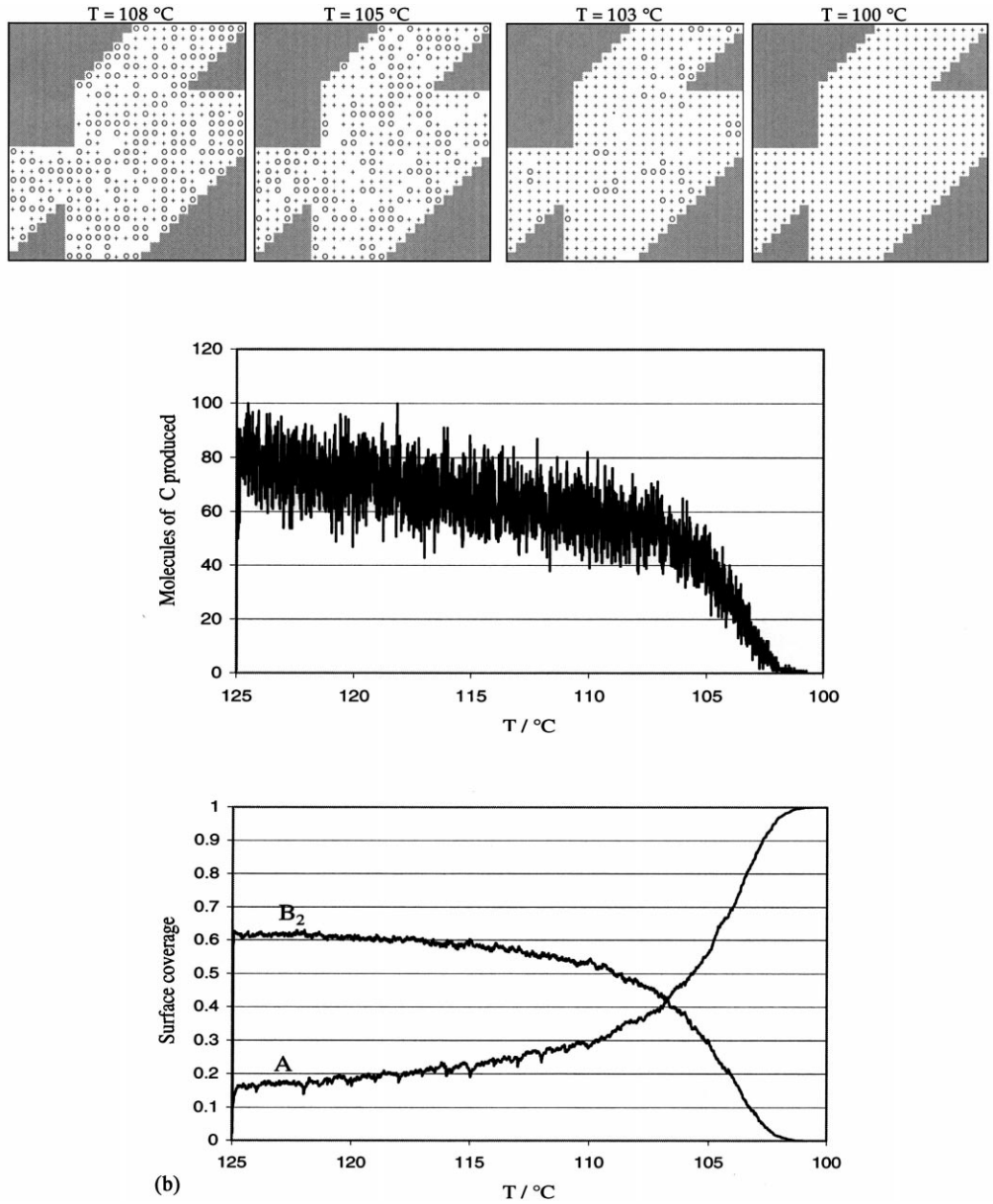

Fig. 2. (*Continued*).

for the increasing (Fig. 2a) and decreasing (Fig. 2b) ramp of the TPR. Fig. 2 also shows four small maps depicting a crystallite surface coverage at different temperatures. The gray color in these maps represents the support, (+) is for A covered sites, (O) is for oxygen covered sites and white is for empty sites.

During the increasing part of the TPR before 112°C, the catalyst surface is covered mainly by A (see map at 112°C). This inhibits B_2 adsorption resulting in very small production of C corresponding to a low steady state. In addition to the different structural sites, defects sites randomly located on the corners and edges were introduced in the program. The desorption of A in the defects sites occurs at a preset temperature selected to match experimental results (Qin and Wolf, 1995,a,b), otherwise if uniform activity is assumed, higher temperatures are required for ignition.

As the temperature continues increasing, species A starts to desorb at the defects sites so that B_2 can adsorb and react with adsorbed A (see map at 113°C). Desorption of A initiated at the defect sites breaks the layer of adsorbed A in a rapid process, similar to ignition (∼113°C), that propagates to the whole crystallite, as it can be seen in the map at 115°C. After the high coverage of A is removed, the surface stays at a high steady state with a lower A coverage and a steady production of C (see map at 117°C). After ignition, the temperature continues increasing up to 130°C but it does not affect significantly the surface coverage or C production

Table 2
Rate parameters used during simulations

Simulation #	Adsorption			Desorption			Surface reaction		
	f_0^1	f_1^1	f_2^1	f_0^2	f_1^2	f_2^2	f_0^3	f_1^3	f_2^3
MC0	1	1	1	1	1	1	1	1	1
NN0	1	1	1	1	1	1	1	1	1
S1	1.99	1	1	1	1	1	1	1	1
S2	1.99	1	1.5	1	1	1	1	1	1
S3	1.99	1.5	1.5	1	1	1	1	1	1
S4	1.99	1.99	1.99	1	1	1	1	1	1
S5	0.1	1	1	1	1	1	1	1	1
S6	0.1	1	0.5	1	1	1	1	1	1
S7	0.1	0.5	0.5	1	1	1	1	1	1
S8	0.1	0.1	0.1	1	1	1	1	1	1
D1	1	1	1	100	1	1	1	1	1
D2	1	1	1	100	100	100	1	1	1
R1	1	1	1	1	1	1	100	1	1
R2	1	1	1	1	1	1	100	1	10
R3	1	1	1	1	1	1	100	10	10
R4	1	1	1	1	1	1	100	100	100
R5	1	1	1	1	1	1	0.01	1	1
R6	1	1	1	1	1	1	0.01	1	0.1
R7	1	1	1	1	1	1	0.01	0.1	0.1
R8	1	1	1	1	1	1	0.01	0.01	0.01

because the coverage of B_2 reaches the limiting requirement stated in condition ii) for B_2 adsorption.

Fig. 2b shows the reaction rates and surface coverage changes when the reactor temperature is linearly decreased from 125°C at a rate of −1°C every 100 MC iterations. The upper coverage maps show that as the reactor temperature is decreased, the surface coverage of A gradually increases until it eventually covers the whole surface. The results on one crystallite predict the expected high CO coverage at low temperature and low CO coverage at high temperature, which are the trends experimentally observed by FTIR measurements [32,33,36].

This model restricts the adsorption of B_2 to occur when half of the nearest neighboring sites are occupied by oxygen. This is an important assumption since without it, due to the absence of an oxygen desorption term (or its low rate of desorption), the surface would be eventually fully covered by oxygen as the reactor temperature increases. This leads to extinction of the reaction due to the oxygen poisoning at high temperature, which is in contradiction with experimental results for CO oxidation. The results shown in Fig. 2 demonstrate that this Monte Carlo model simulates well the behavior of the reaction with respect to temperature. Because the model does not include a bi-stable mechanism including variable rates with coverage, no oscillatory behavior is predicted by the model.

To analyze the effect of crystallite size on the production of C, several simulations were carried out using the rate parameters listed in Table 2. Conditions for these simulations are: (i) feed composition 12% B_2, 2%A and 86% inert and (ii) temperature 115°C. The total number of active sites was maintained almost the same by increasing or decreasing the *number* of crystallites on the support. Table 3 shows the proportion of corner sites, base sites, edges and faces for each crystallite as well as the number of sites in each crystallite and the total number of sites. The rates of the various elementary processes in corners, edges and base atoms were changed a certain fraction with respect to the kinetic parameters of the simulation presented in Fig. 2. The kinetic parameters of the face atoms were not changed and were maintained as in the base case simulation. The rate of production of C is presented per unit site and per unit MC iteration (referred hereafter as the production rate). Since the actual time is related to the number of MC iterations [40] and simulations are carried out under isothermal conditions, the production rate is akin to a turnover frequency.

Fig. 3 shows the results in terms of the production rate, after 5000 MC iterations, for the case in which the *adsorption rate parameters* are increased (Fig. 3a) or decreased (Fig. 3b) with respect to the base case (at 115°C) in which the rates are the same for corners, edges and faces (curve MC0). The other cases presented in Fig. 3a correspond to increases in the adsorption rate of 50 and 100% by increasing the sticking coefficient to its maximum value of 1 (see Table 2). As shown in Fig. 3a the simulations predicts that even for the base case, the production rate increases as the crystallites size increases from 8 to 18 Å, but it has little effect on the production rate for larger crystallite sizes. In the base case, the production rate increases with crystallite size even though the rates are the same in all sites. This result is not intuitive and it is due to the fact that the proportion of sites with higher number of nearest neighbors (NN) increases as crystallite size increases (see Table 3). For an adsorbed species the probability of finding an immediate neighbor to react increases as the number of NN grows. The plane sites have a larger proportion of NN than edge and corner sites and this proportion varies with the particle size, hence the probability for reaction is higher for larger crystallites, where the proportion of sites on [1 1 1] plane is

Table 3
Description of crystallites

Crystallite size (Å)	Proportion corner sites	Proportion base sites	Proportion edge sites	Proportion face [1 0 0]	Proportion face [1 1 1]	Amount of sites per crystallite	Number of crystallites used for simulation
8	0.5	0.25	0.125	0	0.125	24	69
10.8	0.182	0.227	0.227	0.091	0.273	66	25
18.8	0.056	0.155	0.183	0.169	0.437	213	8
27	0.03	0.119	0.148	0.222	0.481	405	4

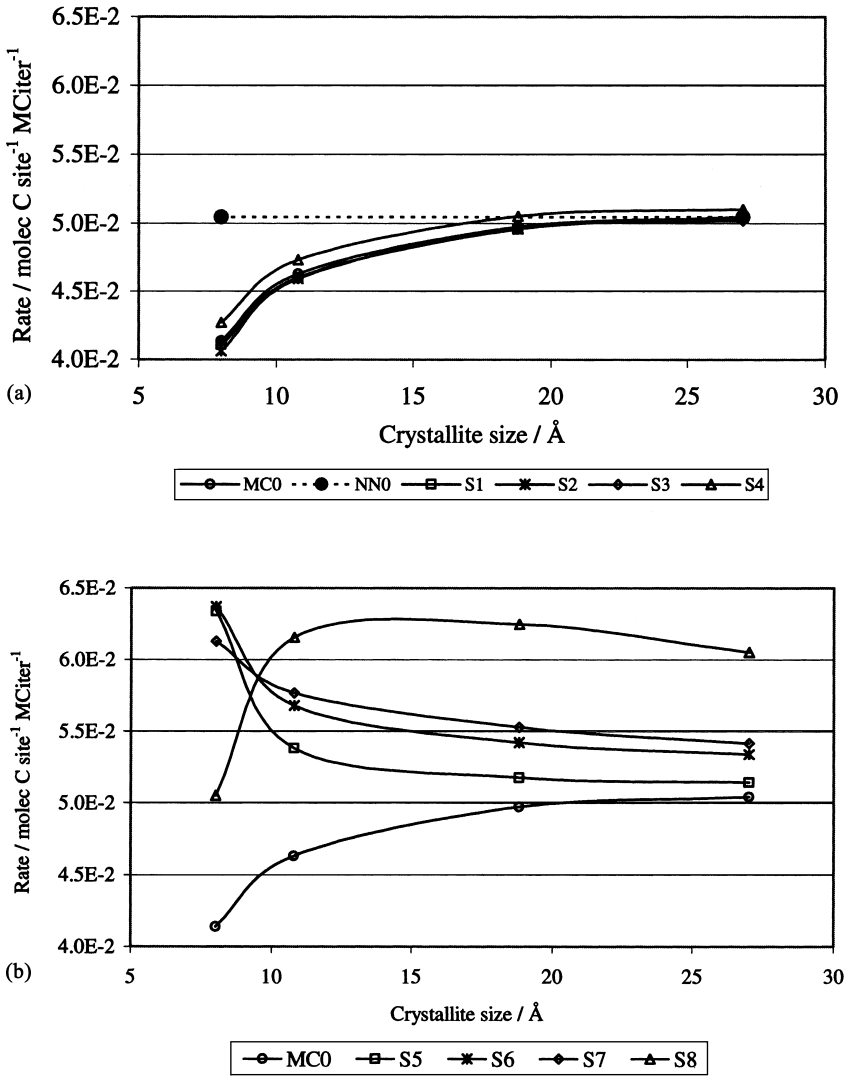

Fig. 3. Production rate versus crystallite size for increases and decreases of the adsorption rate of A relative to the base case (MC0), uniform size. (a) Base case for crystallites with continuous boundary conditions (NN0). Increase in sticking coefficient of A for corners (S1), corners and edges (S2), corners, edges and base sites (S3), same increase in all three sites (S4). (b) Decrease in the sticking coefficient for corners (S5), corners and edges (S6), corners, edges and base sites (S7), same decrease in all three sites (S8). Numerical values are given in Table 2.

the highest. To verify this effect two simulations were carried out considering the smallest and the larger crystallite size with continuous boundary conditions, i.e. all the sites having the same number of NN and same activity. The results of these simulations are shown in Fig. 3a curve NN0. As expected the result shows that, when all the sites have equal number of NN the production rate is not affected by the crystallite size.

Fig. 3a also shows that, in the ranges of values probed, there are little differences when the sticking coefficient increases either in corners (S1) edges (S2) and base sites (S3), and for increases in all these three features (S4). This is due to the fact that adsorption is the process with the largest rate and thus small changes do not affect the production rate significantly.

Fig. 3b, shows that when the rate of adsorption decreases by decreasing the sticking coefficient 10 times with respect to the base case, there are significant increases on the production rate relative to the base case. In this case the rate increases for all cases analyzed but the increase is the highest for the smallest crystallite (about 50%). The production rate enhancement is less significant with increasing crystallite size when the adsorption rate decreases in corners (S5), edges (S6) and bases (S7). The increase in the production rate is due to the fact that as the rate of adsorption decreases, the normalizing denominator used to calculate the probabilities of each event decreases, thus *increasing* the probability of reaction leading to an increase in the production rate of C. The small crystallites have a larger fraction of corner sites, edges and base sites and thus they show the highest increase

in rate. As the crystallite size increases, the proportion of structural features with lower adsorption rate decreases and the rate in the faces predominates over corners edges and base sites. When the adsorption rate decreases in all structural sites (S8), the rate increases even for the larger crystallites because the denominator of the probability function decreases significantly increasing the surface reaction rate for all the sizes analyzed.

For the kinetic parameters used in this simulation, the rate of desorption of A (CO) is orders of magnitude lower than the adsorption and reaction rates at $T = 115^{\circ}$C. Thus variation of desorption rate should not affect significantly the production rate. Fig. 4 shows that this is indeed predicted by the simulation as the results for the various cases (D1 and D2) are superimposed on the results for the base case.

The effect of changes in the surface reaction rates in corners, edges and base sites for various crystallite sizes are shown in Fig. 5a and b. Increasing or decreasing the surface reaction rate decreases the production rate with respect

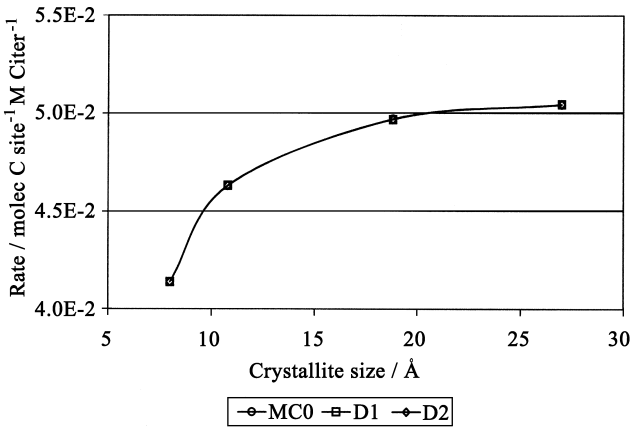

Fig. 4. Production rate versus crystallite size for increases of the rate of desorption of A relative to the base case (MC0), uniform size. D1 = 100-fold increase at corners and D2 = 100-fold increase in all three structural features.

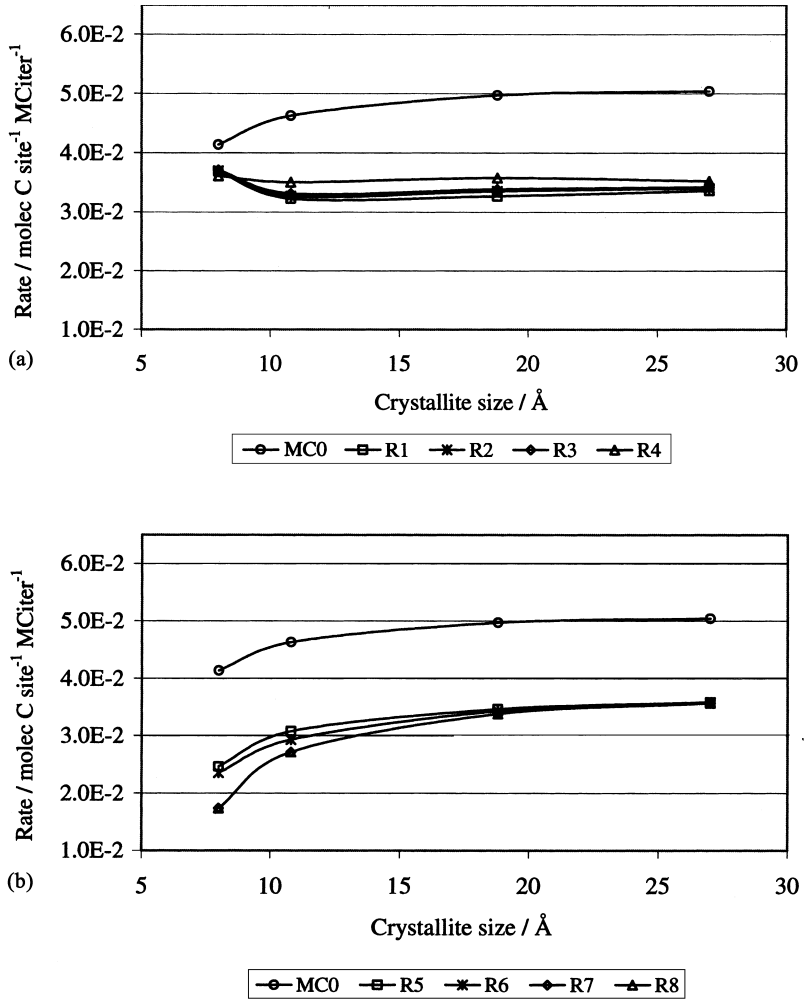

Fig. 5. Production rate versus crystallite size for increases and decreases of the surface reaction rate relative to the base case (MC0), uniform size. (a) Increase in surface reaction rate, at corners (R1), corners and edges (R2), corners, edges, and base sites (R3), same increase in all three sites (R4). (b) Decrease in the surface reaction rate, at corners (R5), corners and edges (R6), corners, edges and base sites (R7), in all three sites the same (R8).

to the base case, but the variation with crystallite size differs for each case. Fig. 5a shows the effect of increasing the reaction rates by two orders of magnitude in the different type of sites (R1, R2 and R3). In this case increasing the surface reaction rate increases the denominator of the probability function thus decreasing the probability of all events to occur. Decreasing the probability of adsorption results in a decrease in the rate of reaction thus resulting in an overall decrease in the production rate. The decrease in production rate is less in the smaller crystallites and becomes independent of size as the crystallite size increases. This is because the smaller crystallites have a larger proportion of structural sites and their rate is then less affected by the assumed changes in the reaction rate.

When the rate of the surface reaction is *reduced* (R5–R8) the denominator of the probability function decreases but the numerator (i.e. the rate) also decreases lowering the surface reaction probability and thus resulting in even lower rates. The effect is more significant in the smallest crystallites because they have the largest proportion of sites in corners and edges and base sites.

3.2. Non-uniform crystallite size distribution

Four different distributions of crystallite size with different averages were chosen with the values and number of crystallites summarized in Table 4. Several cases involving increases and decreases in rate processes are shown in Fig. 6 versus the average crystallite size. The first case corresponds to an increase in the desorption rate in all three structural features (D2). As in the case of the uniform size distribution this has no effect in the production rate. When the sticking coefficients are changed (S4–S8) the trends are also similar to those calculated for the uniform distribution. The rate increases slightly with crystallite size as the sticking coefficient increases (S4) whereas it increases significantly when the sticking coefficient decreases (S5–S8). The increase is slightly less than in the uniform distribution but the trends is similar. The bimodal distribution with an average size of 11 Å, represented by the filled symbols, gives slightly lower rates than the continuous distribution for cases MC0, D2 and S8 but slightly higher values for the cases S5–S7. It is expected that these small differences will decrease as the average size of the bimodal distribution increases. It is interesting regardless if the distribution is

Table 4
Crystallite size distribution and average crystallite size

Distribution	Average crystallite size (Å)	Number of crystallites and sizes (Å)				Total amount of sites
		8	10.8	18.8	27	
Small	8.8	38	5	2	0	1668
Medium	14	3	5	4	1	1659
Large	23.7	0	0	2	3	1641
Bimodal	11	15	1	0	3	1641

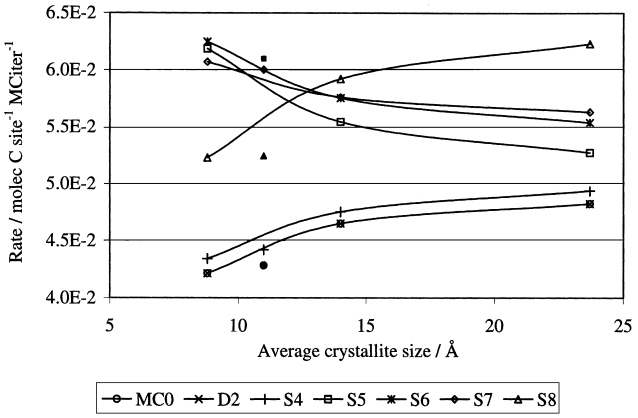

Fig. 6. Production rate versus average crystallite size for increases and decreases of the various adsorption rate processes relative to the base case (MC0), non-uniform size distribution. Filled symbols for a bimodal distribution. Increase in desorption rate D2, increase (S4) and decrease (S5–S8) in the adsorption rate by changes in the sticking coefficients at various sites as specified in Table 2.

uniform or non-uniform, changes in the rates of adsorption and desorption result in similar effects instead of being averaged to a less pronounced effect in the production rate.

The same observations made above between the changes for the uniform and distributed cases are valid when changes in the surface reaction rate are made (R4–R8). Fig. 7 shows these results including the bimodal distribution, which also show trends similar to the non-uniform distribution but slightly lower for all cases analyzed.

The trends predicted by the simulation indicate that the changes in production rate with crystallite size depend on the relative rate of the elementary steps in corners, edges, base sites and faces. The production rate can increase or decrease with crystallite size depending on what rate is higher in the various structural features analyzed. The important

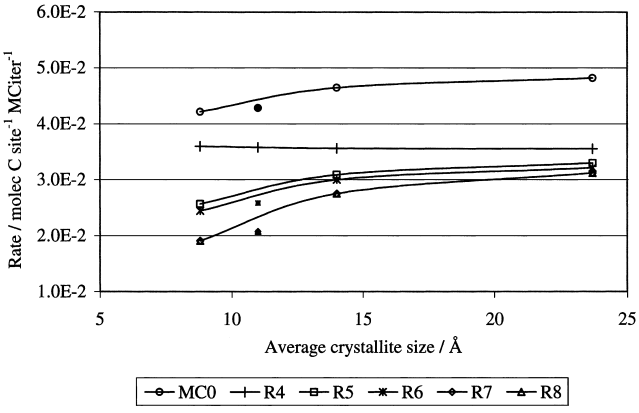

Fig. 7. Production rate versus average crystallite size for increases and decreases of the various reaction rate processes relative to the base case (MC0), non-uniform size distribution. Filled symbols for a bimodal size distribution. Same increase in reaction in all three sites (R4), decrease in reaction rate (R5–R8) at various sites as specified in Table 2.

results predicted by these simulations is that the structural effects of corners edges, base sites and faces due to crystallite size, affect the production rate in ways that depend on which of the elementary steps in the reaction sequence is altered by the presence of these features. In other words there is no universal trend on the effect of crystallite size but it is rather a relative effect that depends on the importance of the interaction of these structural features and the reactants. It should also be stressed that these results are specific to the rate parameters used for the faces in the base case, which were selected on the basis of real experimental conditions. If such conditions are changed, i.e. to higher temperatures, the relative effects presented here will probably change. Work is underway in our group to explore different conditions and ascertain if a general trend emerges on structural effects on catalytic reactions. Monte Carlo simulations provide a way to analyze this effect, not available in continuos models. This method is today at the frontier of the modeling of chemical reacting systems and they will enhance our understanding of fundamental issues in catalytic reactions. Combination of Monte Carlo methods with theoretical results for the elementary processes involved will permit to ascertain the extent of the change in the rate processes that have been parametrically assumed in this work.

Acknowledgements

The support of NSF Grant CTS 99 04033 is gratefully acknowledged.

References

[1] P. Araya, W. Porod, R. Sant, E.E. Wolf, Surf. Sci. 208 (1989) L80.
[2] P. Araya, W. Porod, E.E. Wolf, Surf. Sci. 230 (1990) 245.
[3] K. Binder, D.W. Heerman, Monte Carlo Simulations in Statistical Physics, Solid State Series, Springer, Berlin, 1997.
[4] Y. Boudeville, E.E. Wolf, Surf. Sci. Lett. 297 (1993) L127.
[5] H. Conrad, Gl Ertl, J. Kuppers, Surf. Sci. 76 (1978) 323.
[6] O. Dulub, W. Hebenstreit, U. Diebold, Phys. Rev. Lett. 84 (2000) 3646.
[7] J.A. Dumesic, D.F. Rudd, L.M. Aparicio, J.E. Rekoske, A.A. Tervino, The Microkinetics of Heterogeneus Catalysis, America Chemical Society, Washington, DC, 1992.
[8] G. Ertl, P.R. Norton, J. Rustig, Phys. Rev. Lett. 49 (1982) 177.
[9] G. Ertl, Adv. Catal. 37 (1990) 213.
[10] G. Ertl, Science 254 (1990) 1750.
[11] G.B. Fisher, B.A. Sexton, J.L. Gland, J. Vac. Sci. Technol. 17 (1980) 144.
[12] C.R. Henry, Surf. Sci. Rep. 31 (1998) 231.
[13] R.K. Herz, S.P. Marin, J. Catal. 65 (1980) 281.
[14] A.P.J. Jansen, J.J. Lukkien, Catal. Today 53 (1999) 259.
[15] H.-P. Kaukonen, R.M. Nieminen, J. Chem. Phys. 91 (1989) 4380.
[16] J. Kellow, E.E. Wolf, Chem. Eng. Sci. 45 (1990) 2597.
[17] J. Kellow, E.E. Wolf, Catal. Today 9 (1991) 47.
[18] J. Kellow, E.E. Wolf, AIChE J. 37 (1991) 1844.
[19] S. Ladas, R. Imbihl, G. Ertl, Surf. Sci. 219 (1989) 88.
[20] M.A. Liauw, J. Ning, D. Luss, J. Chem. Phys. 104 (1996) 5657.
[21] M.A. Liauw, P.J. Plath, N.I. Jaeger, J. Chem. Phys. 104 (1996) 6530.
[22] S.J. Lombardo, A.T. Bell, Surf. Sci. Rep. 13 (1991) 1.
[23] J.J. Lukkien, J.P.L. Segers, P.A.J. Hilbers, R.J. Gelten, A.P.J. Jansen, Phys. Rev. E 58 (2) (1998) 2598.
[24] J. Mai, W. von Niessen, A. Blumen, J. Chem. Phys. 93 (1990) 3685.
[25] M. Mavrikakis, P. Stolze, J.K. Nørskov, Catal. Lett. 64 (2000) 101.
[26] R.W. McCabe, L.D. Schmidt, Surf. Sci. 66 (1977) 101.
[27] A.S. McLeod, L.F. Gladden, Catal. Lett. 43 (1997) 189.
[28] A.S. McLeod, L.F. Gladden, J. Catal. 173 (1998) 43.
[29] A.S. McLeod, L.F. Gladden, J. Chem. Phys. 110 (8) (1999) 4000.
[30] A.S. McLeod, Catal. Today 53 (1999) 289.
[31] H. Persson, P. Thormählen, V.P. Zhdanov, B. Kasemo, Catal. Today 53 (1999) 273.
[32] F. Qin, E.E. Wolf, Chem. Eng. Sci. 50 (1995) 117.
[33] F. Qin, E.E. Wolf, Ind. Eng. Chem. Res. 34 (1995) 2923.
[34] F. Qin, L. Tagliablue, L. Piovesan, E.E. Wolf, Chem. Eng. Sci. 53 (5) (1998) 919.
[35] B.C. Sales, J.E. Turner, M.B. Maple, Surf. Sci. 103 (1981) 54.
[36] R. Sant, D. Kaul, E.E. Wolf, Chem. Eng. Sci. 45 (1990) 3137–3147.
[37] Fl Schuth, B.E. Henry, L.D. Schmidt, Adv. Catal. 39 (1993) 51.
[38] M.M. Slinko, N.I. Jaeger, Oscillating Heterogeneous Catalytic Systems, Elsevier, Amsterdam, 1994.
[39] R. Van Hardeveld, F. Hartog, Surf. Sci. 15 (1969) 189.
[40] D.G. Vlachos, F. Schuth, R. Aris, L.D. Schmidt, Physica A 188 (1992) 302.
[41] E. Wicke, P. Kummann, W. Keil, J. Schiefler, Ber. Bunsenges. Phys. Chem. 84 (1980) 315.
[42] G.R. Wilson, W.K. Hall, J. Catal. 17 (1970) 190.
[43] G.R. Wilson, W.K. Hall, J. Catal. 24 (1972) 306.
[44] V.P. Zhdanov, B. Kasemo, Surf. Sci. 405 (1998) 27.
[45] V.P. Zhdanov, Surf. Sci. 426 (1999) 345.
[46] V.P. Zhdanov, B. Kasemo, Surf. Sci. Rep. 39 (2000) 25.
[47] R.M. Ziff, E. Gulari, Y. Barshad, Phys. Rev. Lett. 56 (1986) 2553.